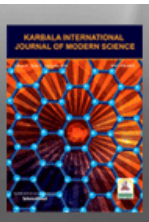

Karbala International Journal of Modern Science

Volume 8 | Issue 3 Article 22

Purifications of Iraqi Petroleum Using Ceramic Ball Nano Cobalt Nickel Ferrite Filter

Huda Jabbar
Department of Applied Sciences, University of Technology, Huda.J.abdulhussein@uotechnology.edu.iq

Enas Muhi
Department of Applied Sciences, University of Technology

Tahseen Hussien
Department of Physics, University of Diyala- Iraq

Recommended Citation

Jabbar, Huda; Muhi, Enas; and Hussien, Tahseen (2022) "Purifications of Iraqi Petroleum Using Ceramic Ball Nano Cobalt Nickel Ferrite Filter," *Karbala International Journal of Modern Science*: Vol. 8 : Iss. 3 , Article 22.
Available at: https://doi.org/10.33640/2405-609X.3252

Purifications of Iraqi Petroleum Using Ceramic Ball Nano Cobalt Nickel Ferrite Filter

Abstract

Iraqi petroleum, especially from the Al-Ahdab, has a big problem resulting from its high percentage of heavy metals. In this paper, heavy metals were reduced or removed from Iraqi petroleum using a Ceramic Ball Nano Cobalt Nickel Ferrite Filter (BCNF), synthesized by combining kaolin and palm frond in a 30% ratio with Co0.8Ni0.2Fe2O4 nanoparticles in a various ratios (5, 10, 15, and 20%). The sol-gel technique prepared Co0.8Ni0.2Fe2O4 nanoparticles. The structure and magnetic properties of the material are described using X-RD, FT-IR, and VSM techniques. In addition, the water ab-sorption ratio and apparent porosity were assessed. The results show that the ceramic ball Nano cobalt-nickel ferrite filter reduces V, Ni, and Fe in crude petroleum. As a result, heavy oil has been converted to the lightest petroleum obtainable. These filters will also become more popular because of their low preparation costs, ease of preparation, and ability to remove crude petroleum.

Keywords

Nano ferrite; Kaolin; magnetic ceramic filter; Porosity; purifying Crude petroleum

RESEARCH PAPER

Purifications of Iraqi Petroleum Using Ceramic Ball Nano Cobalt Nickel Ferrite Filter

Huda Jabbar [a,*], Enas Muhi [a], Tahseen Hussien [b]

[a] Department of Applied Sciences, University of Technology, Iraq
[b] Department of Physics, University of Diyala, Iraq

Abstract

Iraqi petroleum, especially from the Al-Ahdab, has a big problem resulting from its high percentage of heavy metals. In this paper, heavy metals were reduced or removed from Iraqi petroleum using a Ceramic Ball Nano Cobalt Nickel Ferrite Filter (BCNF), synthesized by combining kaolin and palm frond in a 30% ratio with $Co_{0.8}Ni_{0.2}Fe_2O_4$ nanoparticles in a various ratios (5, 10, 15, and 20%). The sol−gel technique prepared $Co_{0.8}Ni_{0.2}Fe_2O_4$ nanoparticles. The structure and magnetic properties of the material are described using X-RD, FT-IR, and VSM techniques. In addition, the water absorption ratio and apparent porosity were assessed. The results show that the ceramic ball Nano cobalt-nickel ferrite filter reduces V, Ni, and Fe in crude petroleum. As a result, heavy oil has been converted to the lightest petroleum obtainable. These filters will also become more popular because of their low preparation costs, ease of preparation, and ability to remove crude petroleum.

Keywords: Nano ferrite, Kaolin, Magnetic ceramic filter, Porosity, Purifying crude petroleum

1. Introduction

The primary source of energy in Iraq is crude oil [1]. The presence of heavy metals such as vanadium, lead, nickel, iron, cobalt, and zinc in crude oil, particularly from the Al-Ahdab well in Kut Province, is a significant issue. It has also been listed as a heavy crude oil well. However, its ability to accelerate distillation tower and turbine corrosion is of great concern to the petroleum industry and the environment [2,3]. Some of the metal removal methods from crude oil include asphalting [4], hydrocracking, and hydrotreating [5]; other methods of study include oxidation [6], adsorption [7], and acid attack, extraction [8]. Nanotechnology is currently one of the most rapidly emerging science and technology sectors, bridging many traditional divides. When the size of adsorbents is lowered to the Nano size range, the surface area and capacity of nanoparticles in adsorption processes increase [9]. Hassan et al. used iron oxide to crack and adsorb asphaltene molecules [10]. By utilizing nickel oxide nanoparticles, Benjumea et al. have reported asphaltene adsorption, kinetics, and thermodynamic equilibrium [11]. Nazila et al. synthesized hematite "α-Fe_2O_3″ and maghemite "γ-Fe_2O_3″ nanoparticles for the adsorption and removal of asphaltene from the prepared solution. The result showed that maghemite "γ-Fe_2O_3″ is more efficacious [12]. Ali et al. synthesis (NFNs) was then used as an adsorbent for the removal of heavy metals [13]. Several studies have used ceramic filters as oil purifiers [14]. One of the benefits of using ceramic materials as a filter is their thermal stability, corrosion resistance, strong chemical resistance, high permeability, and conductivity, among other things [15,16]. Porous ceramic filters have been used in various separation and filtering procedures, including diesel particulate filtration, filtration of liquids, and water filtration [17,18]. Using asymmetric ceramic membranes with pore sizes of 500 nm, Ashrafizadeh et al. filtered asphaltenes from crude petroleum [19]. For ultrafiltration extraction of asphaltene from crude oil, Kazemi et al. developed a crude petroleum filter

Received 16 April 2022; revised 19 June 2022; accepted 20 June 2022.
Available online 1 August 2022

* Corresponding author at:
E-mail address: Huda.J.abdulhussein@uotechonolgy.edu.iq (H. Jabbar).

https://doi.org/10.33640/2405-609X.3252

constructed of aluminum oxide nanoparticles (Al_2O_3) with a pore size of 200 nm [20]. Therefore, the object of the research is to obtain light crude petroleum by eliminating or reducing these elements and obtaining outcomes that are as close to the criteria as possible. The filter is low-cost and has a low sintering temperature because it is made of naturally occurring raw materials. We selected kaolin ball clay as the pore-forming material during sintering since it is a representative and affordable natural resource from Iraq. Next, Co–Ni ferrite nanoparticles were synthesized using the sol–gel process, which is easy and low-cost. After examining the microstructure, physical, mechanical, and magnetic properties of the filter, we investigated how adding Co–Ni ferrite nanoparticles would change them.

2. Materials and methods

2.1. Synthesis of Ni–Co nano ferrite and synthesis filters

The raw materials for this study were crude petroleum received from Al-Ahdab Oil Refinery, Kut, and kaolin collected in Iraq from the western desert (Dwekhla), with the chemical analysis of kaolin powder listed in Table 1. Natural additive (palm frond) obtained locally with a 30% ratio, milled, sieved to obtain a nanoparticle size (300 nm), and kaolin added. Sol–gel auto combustion was used to create a stoichiometric formulation of $Co_{0.8}Ni_{0.2}Fe_2O_4$ cobalt-nickel ferrite nanoparticles (CNF). The solution that contains the desired stoichiometric solution of Co, Ni, and Fe nitrates is a mixture with citric acid at a molar ratio of 1:1. It was neutralized at 9. at 80 °C. The solution was stirred on a magnetic stirrer until it thickened and gradually turned into a gel and heated to (285 °C). Added $Co_{0.8}Ni_{0.2}Fe_2O_4$ nanoparticles at ratios of 5, 10, 15, and 20% to the mixture (kaolin and palm frond) (see Table 2). Following the mixture of the specimens, they sintered at 1100 °C.

2.2. Characterizations

The crystalline phases of synthesized specimens were studied using x-ray diffraction "XRD"; type ADX-2500, Japans equipped with a Cu kα radiation source and a wavelength of 1.54060 Å. To confirm the spinel structure of the specimens, Fourier transforms infrared spectroscopy was performed on all of them with a Shimadzu IRAffinity-1, "FT-IR" spectrometer from Japan in the range of 300–4000 cm^{-1} using KBr pellets. All filters were tested for magnetic properties at room temperature using a vibrating specimen magnetometer "VSM" and an (LBKFB model Meghnatis Daghigh Kavir Company).

Table 2. Composition ratios of prepared (BCNF) filters.

Code of specimen	Kaolin + palm frond (P.F) content wt%	CNF content wt%
M1	100	0
M2	95	5
M3	90	10
M4	85	15
M5	80	20

3. Ceramic ball nano cobalt nickel ferrite filter test

3.1. Apparent porosity, water absorption, and compressive strength

Apparent Porosity (A.P.%) and Water Absorption (W.A.%) of the specimens were calculated using the Archimedes method and ASTM standards (C373) and calculated by Equations (1) and (2) [21]:

$$(\text{A.P.})\% = \frac{\text{Ws} - \text{Wd}}{\text{Ws} - \text{Wi}} \times 100\% \quad (1)$$

$$(\text{W. A.})\% = \frac{\text{Ws} - \text{Wd}}{\text{Wd}} \times 100\% \quad (2)$$

W_s: The mass of a specimen immersed in water (g), W_d: The dried specimen's mass (g), W_i: Suspended mass (g).

The Compressive Strength (C.s) of all specimens was determined following ASTM (C1116) by using the formulae [22]:

$$\text{Cs} = \frac{\text{F}}{\text{A}} \quad (3)$$

F: Applied load (N), and A: Area of the specimens (mm^2).

3.2. Adsorption of metals ions and removal efficiency

Metal concentrations in crude petroleum range from a few ppm to over (1000) ppm [23]. The Spectr

Table 1. Chemical Composition for kaolin.

Oxides	sio_2	Al_2o_3	Fe_2o_3	Cao	Tio_2	K_2O	Na_2o	Mgo	Loss on ignition%
Kaolin wt. %	49.38	32.72	2.07	1.19	1.08	0.44	0.22	0.18	12.42

oil M, a standard device for fuel investigation, is used to assess metal adsorption. The spectrometer is notable for its portability, durability, and ease of use. It was designed particularly for the investigation of gasoline and oil specimens. Rotating disc electrode method "RDE," ASTM (D-6728) is used to examine minute amounts of dissolved or suspended contaminant particles in a fuel sample and metals such as (Ni, Na, V, Ca, Mg, Zn, Mn, Si, Cr, Al, Fe, C, and Pb). The removal efficiency (η) was calculated by using Equation (4) [24]:

$$\eta = \frac{Co - Ce}{Co} \times 100\% \quad (4)$$

C_o, C_e initial metals concentration before and after treatment (mg/L) respectively.

4. Results

4.1. Analyzed structure

Figure (1) demonstrates the X-Ray diffraction of the synthesized products. The major phase of the specimen (M1) is mullite, and the cristobalite phase is the second phase since it contains a lot of kaolin, which means it has a lot of mullite. XRD patterns of a ceramic filter with $Co_{0.8}Ni_{0.2}Fe_2O_4$ ratios (5, 10, 15, and 20) %, which show the presence of $Co_{0.8}Ni_{0.2}Fe_2O_4$ in these ceramic filter causes crystalline peaks. Because the $Co_{0.8}Ni_{0.2}Fe_2O_4$ nanoparticles dispersed in the ceramic ball. Specimens (M2,M3, M4,M5) presented the mullite, cristobalite phases and cubic spinel structure of $Co_{0.8}Ni_{0.2}Fe_2O_4$ with seven peaks (311), (222), (400), (422), (511), (440) and (622), located at 2θ = 35.64°, 37.28°, 43.39°,53.72° ,57.23°,62.91° and 74.56° respectively. It can be seen that the most intense peak is (311) in all specimens. In addition, as the $Co_{0.8}Ni_{0.2}Fe_2O_4$ concentration was increased, the intensity of the peak, particularly the favored plane, increased, whereas the intensity of the mullite phase was reduced due to lower kaolin raw. The addition of $Co_{0.8}Ni_{0.2}Fe_2O_4$ to porous ceramic may have resulted in the atrophy of some phases.

Figure (2) demonstrates the FT-IR spectrum of (BCNF) filters. The peak observed in the range (486.0616–493.7768 cm^{-1}) is attributed to the octahedral complexes while the peaks observed in the range (561.2854–569.0007 cm^{-1}) are attributed to tetrahedral complexes, which indicated the spinal structure of $Co_{0.8}Ni_{0.2}Fe_2O_4$ in the ceramic filter. The bands observed in the range (798.25–909.87 cm^{-1}) are attributed to AL-O stretching and the peak at (1070.53 cm^{-1}) is anti-symmetric stretching vibrations of the Si–O–Si in amorphous silica and Si–O–Al networks. The bands are located at (1095.53 cm^{-1}) for specimen, (1128.39 cm^{-1}) for 5% $Co_{0.8}Ni_{0.2}Fe_2O_4$, 10% $Co_{0.8}Ni_{0.2}Fe_2O_4$, (1130.32 cm^{-1}) for 15% $Co_{0.8}Ni_{0.2}Fe_2O_4$ and (1126.47 cm^{-1}) for 20% $Co_{0.8}Ni_{0.2}Fe_2O_4$ attributed to C–O stretching. The CO_2 absorption was observed at around (1519.59–1557.47 cm^{-1}). The band about (3664.75 cm^{-1}) as the specimen where the peak located at range (3748.28–3754.45 cm^{-1}) attributed to Si–O–H vibration. The aliphatic and aromatic C–H stretching bonds are responsible for the band detected at (2360.23–2365.65 cm^{-1}). C–H stretching bands are responsible for further peaks in the range (2852.23–2945.06 cm^{-1}). The stretching vibration of the hydroxyl group is responsible for the faint peaks seen in the region (3444.98–3680.41 cm^{-1}). The FTIR spectrum of the (BCNF) filter specimens is shown in Table 3.

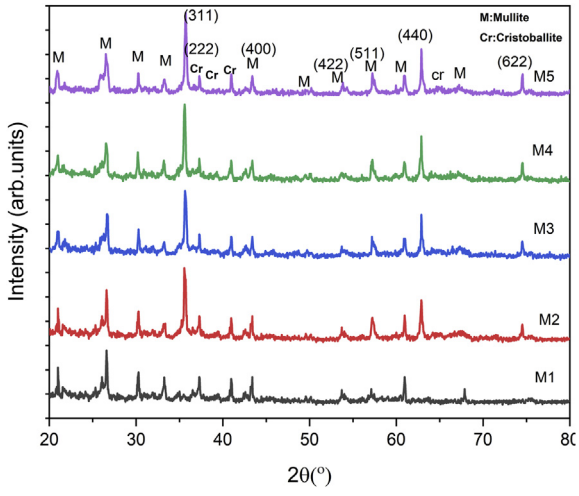

Fig. 1. The XRD pattern of (BCNF) filters.

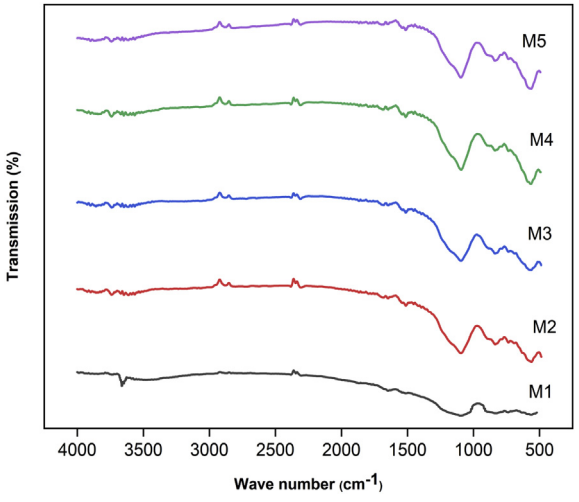

Fig. 2. FT-IR spectrum of (BCNF) filters.

Table 3. FT-IR spectral bands of (BCNF) filters.

Specimen	Weight ratio	FTIR frequency bands (cm^{-1})	
		ν_1	ν_2
M1	0	–	–
M2	5	561.2854	486.0616
M3	10	565.1430	487.9904
M4	15	567.0719	491.84808
M5	20	569.0007	493.7768

4.2. Microstructure

FE-SEM micrograph was used to examine the surface morphology of the specimens. Figure 3(a) shows surface FE-SEM micrographs of the prepared filters. The filter appears to be made up of grains that are heterogeneously distributed, as well as large and small grains. The high calcination temperature of 1100 °C is responsible for the large and inhomogeneous distribution of grain sizes. Pores of such order and homogeneity, as well as the magnet's small weight, may be ideal for a variety of applications. $Co_{0.8}Ni_{0.2}Fe_2O_4$ nanoparticles with a spherical form were equally dispersed on the surface or inserted between layers of the crystal mullite, as shown in Fig. 3 (b).

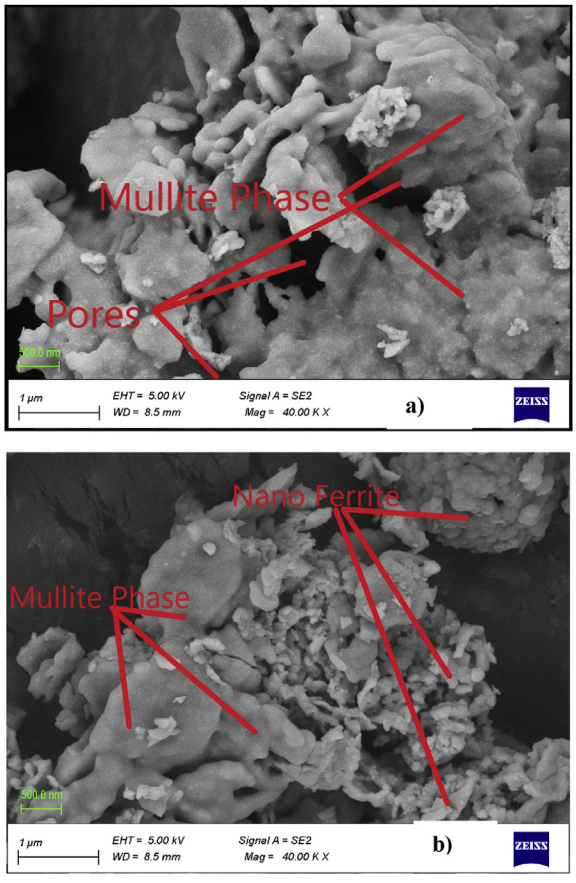

Fig. 3. FE-SEM micrographs of (BCNF) filters a) M1, b) M5.

4.3. Magnetic measurements

Magnetic hysteresis loops at room temperature were used to assess the magnetic characteristics of (BCNF) filters. The magnetic properties of (BCNF) filters are determined by the ferrite phase's magnetic properties and the degree of connection between the two phases. As a result, non-magnetic mullite, cristobalite phases, and interface effects alter the magnetic properties of the ceramic filter by changing the distribution of magnetic ions and their spin distribution, notably at the heterointerface, and therefore the magnetic interaction. The insertion of $Co_{0.8}Ni_{0.2}Fe_2O_4$ nanoparticles into the ceramic filter is expected to create changes in the magnetic properties of the materials. The values of Ms, Mr, Hc, and Mr/Ms are listed in Table 4. The coercivity (Hc) and magnetization (Ms) increase with increasing $Co_{0.8}Ni_{0.2}Fe_2O_4$ nanoparticles content. Because of the increasing magnetic dipoles and considerable alignment along the applied field, the magnetization and coercivity increase from (0.0.215–9.76emu/g) (371.05–1159.7Oe), respectively (see Fig. 4).

4.4. Apparent porosity and water absorption

Figure (5) shows the effect of $Co_{0.8}Ni_{0.2}Fe_2O_4$ nanoparticles' addition on the apparent porosity and water absorption. The maximum apparent porosity was

Table 4. Magnetic parameters of (BCNF) filters.

Specimen	M_s (emu/g)	M_r (emu/g)	H_C (Oe)	M_r/M_s
M1	.....	.....	.....	.....
M2	0.215	0.0043	371.05	0.02
M3	0.612	0.3167	1073.45	0.517
M4	2.88	1.5796	1122.4	0.548
M5	9.76	5.1025	1159.7	0.522

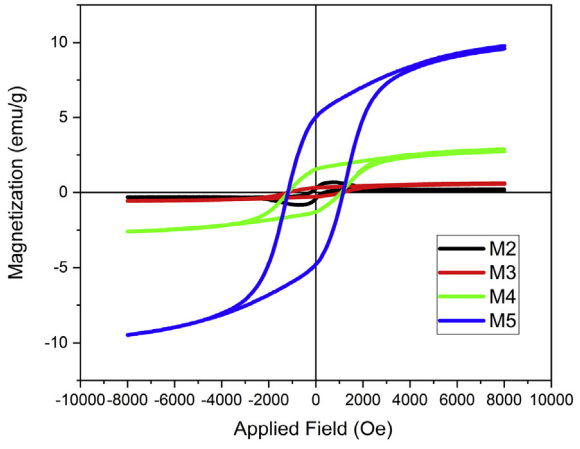

Fig. 4. VSM behavior of (BCNF) filters.

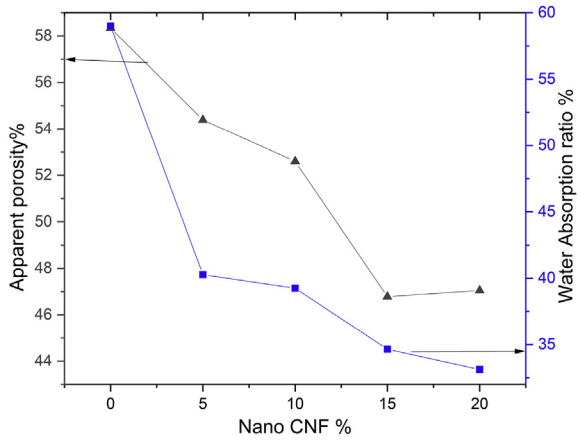

Fig. 5. Effect of ($Co_{0.8}Ni_{0.2}Fe_2O_4$) ratios on the apparent porosity and water absorption of (BCNF) filters.

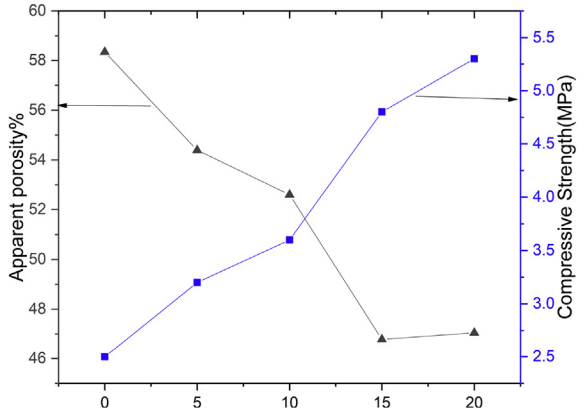

Fig. 6. Effect of ($Co_{0.8}Ni_{0.2}Fe_2O_4$) ratios on the porosity and compressive strength of prepared filter.

58.34% without any addition of $Co_{0.8}Ni_{0.2}Fe_2O_4$ nanoparticles, while the minimum apparent porosity was recorded to be 47.05% at 20 wt.% of $Co_{0.8}Ni_{0.2}Fe_2O_4$ nanoparticles. The water absorption decreases almost linearly from 59% to 33.12% by increasing the wt.% of $Co_{0.8}Ni_{0.2}Fe_2O_4$ nanoparticles from 0 to 20 wt.%. The difference in porosity is due to the distribution and agglomeration of nano additives [10]; Because $Co_{0.8}Ni_{0.2}Fe_2O_4$ nanoparticles employed as a filler shut some pores, the use of nanoparticles reduces porosity. These tend to decrease water absorption. These behaviors agree with Hanoon [25]. Due to the high surface area of the nanoparticles, the adsorption capacity increased even though the porosity dropped.

4.5. Compressive strength

As more nanoparticles are added, the compressive strength values increase, and this impact is considerably more pronounced when $Co_{0.8}Ni_{0.2}Fe_2O_4$ is added. The compressive strength of the ceramic filter is increased by 27% by adding 15 wt.% of $Co_{0.8}Ni_{0.2}Fe_2O_4$ nanoparticles to 20 wt.%. In general, nanoparticles improve a specimen's strength by pinning dislocations, reducing porosity, and increasing resistance to plastic deformation [25] (see Fig. 6).

4.6. Adsorption of metals ions

The adsorption studies were carried out to verify the adsorption capabilities of the (BCNF) filters, which were designed to remove heavy metals from

Table 5. Remove heavy metals from AL-Ahdab Crude Petroleum after treatment (BCNF) filter (M3).

Metallic Content	Value Crude Petroleum (ppm)	Crude Petroleum after immersion in magnetic ceramic filter balls at(7 days)	Crude Petroleum after immersion in magnetic ceramic filter balls at(14 days)	Crude Petroleum after immersion in magnetic ceramic filter balls at(28 days)
V	86	55.78	44.05	40.23
Ni	32	22.26	16.46	10.54
Fe	1.32	0.87	0.25	0.15
Na	0.76	0.21	0.17	0.08
K	0.12	0.03	0.00	0.00
Mg	0.92	0.48	0.37	0.23
Ca	0.48	0.14	0.11	0.06
Pb	0.03	0.00	0.00	0.00
Zn	0.35	0.21	0.14	0.11
Si	0.55	0.40	0.27	0.02
Cr	0.45	0.27	0.20	0.12
Al	3.7	2.23	2.03	1.90
Mn	0.47	0.19	0.05	0.00
Cu	0.11	0.02	0.00	0.00
Li	0.03	0.00	0.00	0.00
C	294 K	269 K	260 K	257 K

Table 6. Comparison between the current study and previous studies.

Specimen	Materials	Cost	Reference
BCNF	Raw materials &Nano ferrite	low cost and readily available materials (kaolin, palm fronds)	This study
NFN's	Nano Ferrite	low	(Ali et al., 2021) [13]
TiO_2, and SiC	Advance materials	high	(Nagasawa et al., 2020) [27]
Nano AL_2O_3	Advance materials	high	(Kazemi et al., 2017) [20]

crude petroleum. Table 5 shows that increasing the immersion time from 7 to 28 days significantly improves the ability to remove metal ions from crude petroleum. After 28 days, about 20%–90% of the metal ions have been removed. The adsorption of metal ions increased rapidly, and with an extended operating duration, a modest rise in elimination was observed. The progressive rise in metal ion adsorption might be explained by the increased availability of adsorption sites on the adsorbent. As a result, the absence of slightness implies no active spot on the surface of (BCNF) filters. At 28 days of immersion time, maximum removal values of 40.23 ppm, 10.54 ppm, 0.15 ppm, 0.08 ppm, 0.23 ppm, and 0.00 were achieved for V, Ni, Fe, Na, Mg, and K, respectively (see Table 6).

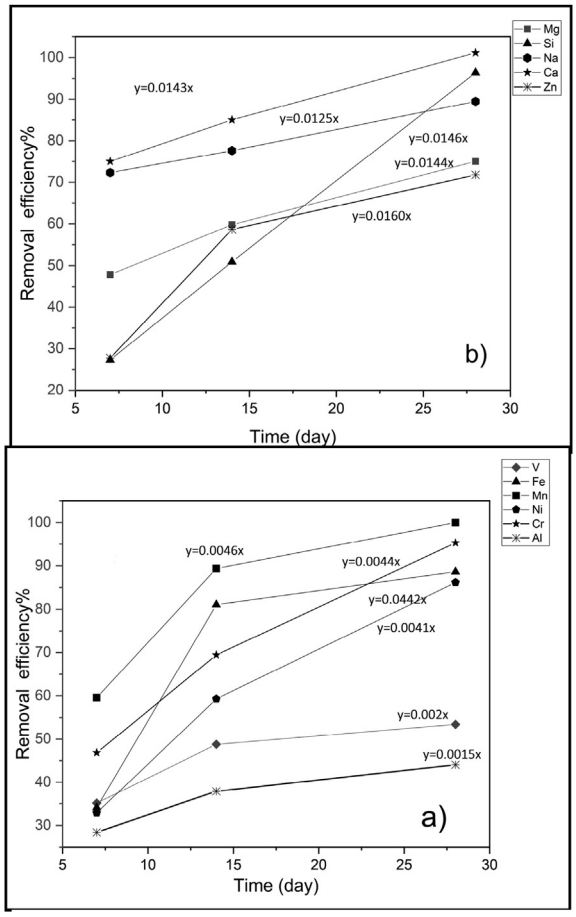

Fig. 7. a), b). Removal efficiency as a function of the contact time of the adsorbent.

4.7. Effect contact time

Contact time is important for heavy metal adsorption by (BCNF) filters. A series of parallel tests were conducted to estimate the equilibrium time for heavy metal adsorption in this study. Figure (7) (a,b) reveals the association between metal removal and adsorbent contact time. As the contact duration was increased, the metal adsorption efficiency improved, and the maximum removal efficiency was reached after 28 days. The results revealed that sorption occurred first, followed by a gradual increase to a time limit, and then progressive equilibration. The sorption is occur because many active sites on the surface of the adsorbent have become complex with metal ions. When the active sites on the surfaces are occupied, the complexation is dominated by the active sites on the pore surface, resulting in the maximum adsorption capacity and adsorption equilibrium [25]. Other studies have found similar adsorption behaviors. According to Salman et al. [26], physicochemical parameters, hydration energy, and diameter play a role in zeolite adsorption capabilities for heavy metal ions.

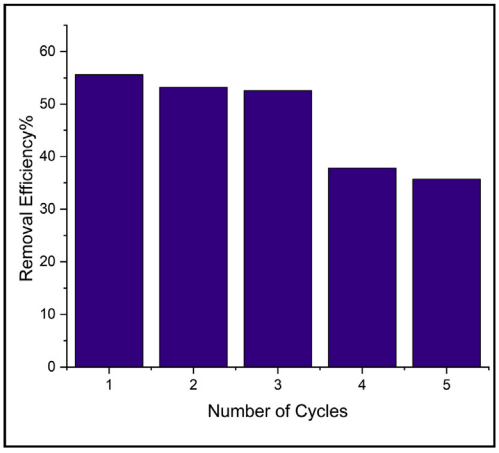

Fig. 8. Reuse (BCNF) filter over five successive adsorption-desorption cycles.

4.8. Recycling of (BCNF) filter

The stability and reusability of the BCNF filter were studied by the adsorption and desorption of heavy metals on the BCNF filter. At each cycle, the metal ion loaded (BCNF) filter recovered by treating with HNO_3 acid was determined to be 0.1 mol/L. The recycled (BCNF) filter is shown in Fig. 8. It can be found that the removal efficiency of the BCNF filter gradually decreases with increasing cycles. The second cycle's adsorption capacity was 53.45 percent lower than the capacity of the original adsorbent in the fourth cycle and remained nearly unchanged in the last cycle. It may be destroying the surface of the BCNF filter by dissolving some cobalt-nickel ferrite particles, indicating that the BCNF filter can be reused for up to three cycles.

5. Conclusion

A novel Ceramic Ball Nano Cobalt Nickel Ferrite Filter (BCNF) was synthesized and combined with a high surface area of kaolin. Furthermore, the magnetic property of nickel cobalt ferrite was manufactured using the sol–gel technique, which was used to remove heavy metals from crude petroleum. The characterization results indicated that the synthesis was productive, the architecture was well-defined, and the magnetism was satisfactory. The maximum adsorption values for vanadium, nickel, and iron were 40.23 ppm, 10.54 ppm, and o.15 ppm, respectively. Removal efficiencies of Si, Ca, Na, Cr, Mg, and Mn was determined 96.38%, 87.53%, 89.46%, 78.09, 75.24%, and 100% respectively. The proposed Ceramic Ball Nano Cobalt Nickel Ferrite Filter had the potential to be used as an effective V, Cr, Fe, Ca, Mn, etc., adsorbent from heavy crude petroleum because of its low cost, high adsorption capacity, and easy recycling features. As a result, heavy oil has been turned into the lightest feasible.

Conflict of interest

There are no financial or other conflicts of interest declared by the authors.

References

[1] M. Barbooti, Evaluation of analytical procedures in the determination of trace metals in heavy crude oils by flame atomic absorption spectrophotometry, Am J Anal Chem. 6 (2015) 23–33.
[2] K. Maher, R. Ibrahim, Improvement of petroleum of Tawke–Zakho crude oil using local clays, J Petrol Gas Expl Res. 2 (2012) 80–86.
[3] S. Naman, K. Maher, R. Ibrahim, Improvement of petroleum of Tawke–Zakho crude oil using local clays, J Petrol Gas Expl Res. 4 (2012) 80–86.
[4] V. Ancheyta, J. Diaz, A review of recent advances on process technologies for upgrading of heavy oils and residual, Fuel. 86 (2007) 1216–1231.
[5] S. Issaka, A. Nour, R. Yunus, Review on the fundamental aspects of petroleum oil emulsions and techniques of demulsification, J Petrol Environ Biotechnol. 6 (2015) 1–15.
[6] C. Flores, V. Cabassud, A hybrid membrane process for Cu(II) removal from industrial wastewater comparison with a conventional process system, Desalination. 126 (1999) 101–108.
[7] K. Smith, W. Lai, Heavy oil microfiltration using ceramic monolith membranes, Fuel. 80 (2001) 1121–1130.
[8] M. Ali, M. Malki, E. Ali, B. Martinie, Deep desulphurization of gasoline and diesel fuels using non- hydrogen consuming techniques, Fuel. 85 (2006) 1354–1363.
[9] J. Konne, K. Opara, Remediation of Nickel from crude oil obtained from Bomu Oil Field using cassava waste water starch stabilized magnetic nanoparticles, Energy Environ Res. 4 (2014) 25–31.
[10] A. Hassan, N. Nassar, L. Carbognani, L. Linares, P. Almao, Iron oxide nanoparticles for rapid adsorption and enhanced catalytic oxidation of thermally cracked asphaltenes, Fuel. 95 (2012) 257–262.
[11] P. Benjumea, C. Franco, E. Patiño, Kinetic and thermodynamic equilibrium of asphaltenes sorption onto nanoparticles of nickel oxide supported on nanoparticulated alumina, Fuel. 105 (2013) 408–414.
[12] N. Shayan, B. Mirzayi, Adsorption and removal of asphaltene using synthesized maghemite and hematite nanoparticles, Energy Fuel. 5 (2015) 1–32.
[13] W. Ali, M. Anwar, Y. Jamal, Synthesis characterization and heavy metal removal efficiency of nickel ferrite nanoparticles (NFN's), Scient Rep. 4 (2021) 11–34.
[14] Y. Dong, J. Zhou, E. Lin, B. Wang, Y. Wang, Reaction-sintered porous mineral-based mullite ceramic membrane supports made from recycled materials, J Hazard Mater. 172 (2009) 180–186.
[15] A. Cescon, J. Qian, Filtration process and alternative filter media material in water treatment, Water. 12 (2020) 3–20.
[16] A. Hasnawy, A. Hashem, Study the effect of changed the sand percentage and its particales size on apparent porosity& comprassive strength of ceramic filters, Al-Qadis J Eng Sci. 7 (2014) 73–90.
[17] Y. Guzman, Certain principles of formation of porous ceramic structures properties and applications, J Por Mat. 9 (2003) 28–33.
[18] M. Okechukwu, N. Arome, Evaluation of a ceramic pot made from local materials as water purification systems, Int J Sci Adv Technol. 6 (2011) 225–233.
[19] S. Ashrafizadeh, M. Ashtari, M. Bayat, Asphaltene removal from crude oil by means of ceramic membranes, J Petrol Sci Eng. 82 (2012) 44–49.
[20] R. kazemi, M. Mirzaei, S. Asghari, J. Ivakpour, Aluminum oxide nanoparticles for highly efficient asphaltene separation from crude oil using ceramic membrane technology, Oil Gas Sci Technol Rev IFP Ener Nouv. 72 (2017) 34–44.
[21] E. Muhi, H. Jabbar, Manufacturing porous ceramic from Iraqi kaolin by using paper pulp, engineering and technology, Journal. 35 (2017) 227–236.
[22] E. Muhi, H. Jabber, Preparation of Ceramic Foam from Porcelanite by using simple direct foaming method, AIP Conf Proc. 212 (2019) 1–9, https://doi.org/10.1063/1.5116934.
[23] H. Jabbar, E. Muhi, T. Hussien, Production ceramic crude petroleum filters from local raw materials, Mater Sci Forum. 1039 (2021) 96–103.
[24] M. Hanoon, A. Al-Attar, A. Resen, The effect of addition of CeO_2 nanoparticles on the microstructure and mechanical properties of Ti-Al-Mg compact samples, Eng Technol J. 36 (2018) 1189–1195.
[25] S. Mustapha, M. Ndamitso, A. Abdulkareem, J. Tijani, A. Mohammed, Potential of using kaolin as a natural

adsorbent for the removal of pollutants from tannery wastewater, Heliyon. 5 (2019), e02923.
[26] S. Halman, H. Shaheen, A. Ghaiath, N. Khalouf, Use of Syrian natural zeolite for heavy metals removal from industrial waste water: factors and mechanism, J Entomol. 5 (2017) 452–546.
[27] H. Nagasawa, T. Omura, T. Asai, M. Kanezashi, Filtration of surfactant-stabilized oil-in-water emulsions with porous ceramic membranes: effects of membrane pore size and surface charge on fouling behavior, J Membr Sci. 2 (2020) 1–34.